Available online at www.sciencedirect.com
ScienceDirect
Trans. Nonferrous Met. Soc. China 26(2016) 319−327
Transactions of Nonferrous Metals Society of China
www.tnmsc.cn

Evolution of secondary phases and properties of 7B04 aluminum alloy during DC homogenization

Li-zi HE[1], Pin-feng JIA[1], Lin ZHANG[2], Jian-zhong CUI[1]

1. Key Laboratory of Electromagnetic Processing of Materials, Ministry of Education, Northeastern University, Shenyang 110819, China;
2. School of Materials Science and Engineering, Northeastern University, Shenyang 110819, China

Received 31 March 2015; accepted 26 August 2015

Abstract: The effects of the direct current (DC) on the evolutions of hardness and morphology of the secondary phases in 7B04 aluminum alloy homogenized at 380−465 °C for 2 h were investigated in detail by electric conductivity measurement, hardness test, X-ray diffraction analysis, field emission scanning electron microscopy and energy dispersive spectrometry. The results show that with increasing temperature from 380 to 465 °C, the electric conductivity of normal homogenized sample decreases from 34.9%IACS to 28.7%IACS, the hardness increases from HV 96 to HV 146, and the area fraction of secondary phase reduces from 4.5% to 1.89%. While, DC homogenized sample has a higher hardness, a lower electric conductivity and a smaller area fraction of secondary phases at the same temperature. The DC enhances the homogenization process by promoting the diffusibility of the solute atoms and the mobility of vacancy.

Key words: 7B04 aluminum alloy; direct current; homogenization; hardness; secondary phase; elemental diffusion

1 Introduction

7B04 aluminum alloy has high strength, low density and good corrosion resistance, and is widely used in aircraft industries [1]. The high mole ratios of Zn to Mg, Cu to Mg and alloying element content of 7B04 alloy endow its attractive combinations of properties, while in turn lead to the difficulty of processing it. The commonly observed secondary phases in as-cast Al−Zn−Mg−Cu alloy are η ($MgZn_2$), T ($Al_2Mg_3Zn_3$) or T ($Al_{32}(Mg,Zn)_{49}$), M ($Mg(Zn_2AlCu)$), S (Al_2MgCu) and $A1_7Cu_2Fe$ [2−4]. A lot of secondary phases remaining in the alloys after the subsequent heat treatment and processing [5−8], approaching to the proximity of composition to the limit of solid solubility in those alloys, could assist the crack initiation, propagation and induce variable properties. FAN et al [6] revealed that a phase transformation of major elements from $Mg(Zn, Cu, Al)_2$ phase to Al_2CuMg phase was found in Al−Zn−Mg−Cu alloy homogenized at 460 °C. The η phase dissolved completely, while T and S phases remained in 7055 alloy heat-treated at 450 °C for 35 h [7].

The electric and magnetic fields provide us new approaches to material preparation and property control. LIU and CUI [8] discovered that the electric field accelerated the dissolution of secondary phase and the decrement in the interdendritic segregation during homogenization, and even suppressed the nucleation of δ' phase during artificial aging. CONRAD [9] demonstrated that an electric current density (>1 kA/cm^2) promoted the transformation of the solid state phase in metals and enhanced the recrystallization rate of cold worked metals, but retarded the subsequent grain growth. ZHOU et al [10] detected that the electric field accelerated the transformation of S phase from type I to type II. HE et al [11] found that the high magnetic field of 12 T promoted the dissolution of both T and S phases in Al−Zn−Mg−Cu alloy during homogenization.

It can be seen that the previous studies mainly focused on magnetic or electric fields, little information on the effects of electric current on mechanical properties and microstructures of aluminum alloy is available. In present work, evolution of the conductivity, hardness and chemical composition of secondary phase in 7B04 alloy during homogenization with applying a DC of 1 kA was

Foundation item: Project (5157406) supported by the National Natural Science Foundation of China
Corresponding author: Li-zi HE; Tel: +86-24-83681760; E-mail: helizi@epm.neu.edu.cn
DOI: 10.1016/S1003-6326(16)64122-5

studied in detail by XRD, FESEM and EDS, and the mechanisms of effects of the DC on the dissolution of secondary phases in 7B04 alloy during homogenization were discussed. The purpose of present work is to find a new heat treatment method for Al−Zn−Mg−Cu alloy.

2 Experimental

The composition of 7B04 alloy is: Al−6.06Zn−2.44Mg−1.57Cu−0.07Si−0.17Fe−0.31Mn−0.14Cr−0.05Ni−0.05Ti (mass fraction, %). The semi-continuous cast ingots with dimensions of 600 mm × 400 mm × 1400 mm were provided by Northeast Light Alloy Co., Ltd., China. Samples with dimensions of 10 mm × 20 mm × 580 mm were sliced from the ingots along the casting direction, and then homogenized at 380, 420, 440 and 465 °C, respectively, for 2 h without or with applying a stable DC of 1 kA, and followed by air cooling. In present work, the homogenization without DC is called normal homogenization, and the homogenization with DC is called DC homogenization. The heating rate was 5 °C/min. A wind bellowing device was used to maintain the temperature variation of sample within ±3 °C. The electric conductivity and hardness of alloy in each condition were the average values of five specimens and measured using a Fischer Sigmascope SMP10 type machine and a 452SVD type hardness tester, respectively.

The secondary phases in as-cast and homogenized alloys were examined by X-ray diffraction analysis (XRD) with Cu $K_{\alpha 1}$ radiation on a PW 3040/60 X diffractometer. Samples for microstructural observations were prepared by the standard metallographic methods and examined on a Zeiss Ultra Plus 60 type field emission scanning electron microscopy (FESEM) equipped with an Oxford AZTEC 50 type energy dispersive X-ray analyzer having an image resolution of 0.8 nm. The area fraction of the secondary phases in as-cast and homogenized alloys was measured by the average of 15 SEM photographs and calculated using Image J software.

3 Results

3.1 Evolution of electric conductivity and hardness during DC homogenization

The electric conductivity and hardness of normal and DC homogenized 7B04 alloys at 380−465 °C for 2 h are displayed in Fig. 1. The hardness and electric conductivity of as-cast alloy are HV 80 and 43%IACS, respectively. The electric conductivity decreases to 34.9%IACS and 33%IACS, respectively, after the as-cast alloy is homogenized at 380 °C for 2 h without and with direct electric current, and then decreases progressively with increasing temperature, and finally achieves 28.7%IACS and 27.7%IACS, respectively, when the alloy is homogenized at 465 °C without and with DC. The hardness increases to HV 96 and HV 106.4, respectively, when the as-cast alloy is homogenized at 380 °C without and with DC, and then increases progressively with increasing temperature, and finally achieves HV 137.5 and HV 146, respectively, when the alloy is homogenized at 465 °C for 2 h without and with DC.

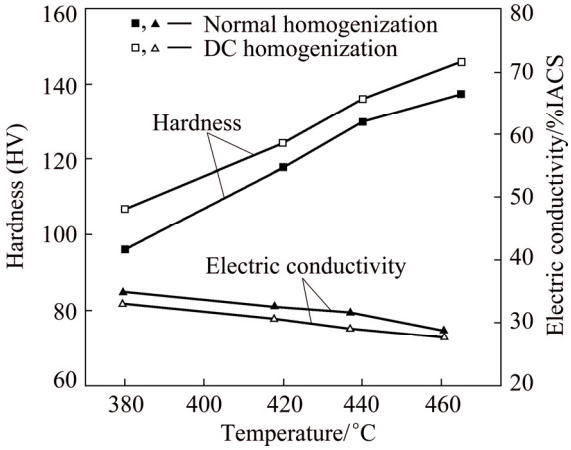

Fig. 1 Electric conductivity and hardness of normal and DC homogenized alloys at 380−465 °C

3.2 Evolution of morphologies of secondary phases during DC homogenization

3.2.1 XRD patterns

The XRD patterns of as-cast and homogenized alloys are shown in Fig. 2. The XRD peaks of α(Al), $MgZn_2$(T), Al_2CuMg(S) and Al_7Cu_2Fe are detected in as-cast 7B04 alloy. With increasing temperature, the amount and height of diffraction peaks of T phase decrease, while those of S phase increase when the

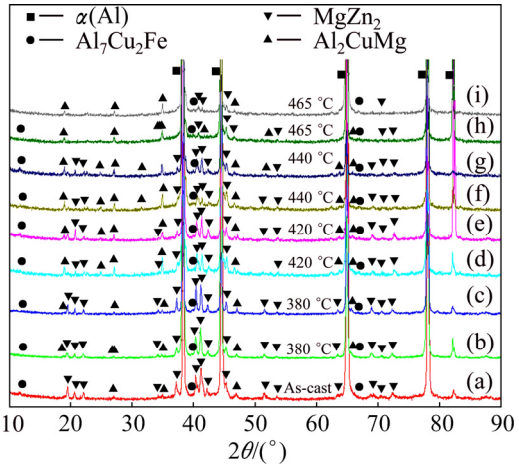

Fig. 2 XRD patterns of as-cast (a) and homogenized alloys (b−i): (b, d, f, h) Normal homogenization; (c, e, g, i) DC homogenization

temperature is not higher 440 °C, and then decrease when the temperature reaches 465 °C. The application of DC further decreases the amount and the peak heights of *T* and *S* phases at the same temperature.

3.2.2 Evolution of compositions of *T* and *S* phases during DC homogenization

The as-cast 7B04 alloy has an average grain size of 115 μm, and a network of the eutectic structure of primary *α*(Al) and secondary phases located at grain and interdendritic grain boundaries (Fig. 3). According to the results of EDS analysis, the secondary phases in as-cast alloy normally contain *T*, *S* and Al_7Cu_2Fe phases, and the compositions of these phases are listed in Table 1, which are similar to those in as-cast 7050 alloy obtained by JIA et al [12].

The morphologies of the secondary phases in homogenized alloys at 380 °C and 465 °C are shown in Fig. 4. With increasing temperature, the coarse eutectics become small, discontinuous and spheroidized, and appear as a necklace-like distribution at grain boundaries. The DC homogenized sample has smaller size and less amount of secondary phases at the same temperature. The evolution of area fraction of secondary phases in homogenized samples at 380−465 °C is demonstrated in Fig. 5. The area fraction of the secondary phase reduces suddenly from 5.47% to 4.5% when the as-cast alloy is homogenized at 380 °C, and then decreases gradually with increasing temperature, and finally reaches 1.89% at 465 °C. With the application of DC, the area fraction of secondary phases decreases rapidly to 4.2% at 380 °C, and then to 1.14% at 465 °C. The DC homogenized sample has smaller area fraction of secondary phases than the normal homogenized sample at the same temperature. The

Table 1 Compositions of secondary phases in as-cast 7B04 alloy obtained by EDS analysis (mass fraction, %)

Phase	Mg	Al	Fe	Cu	Zn
T	13.3−20.0	16.8−30.5	−	27.7−36.7	26.3−35.5
S	10.7	44.4	−	42.3	2.6
Al_7Cu_2Fe	3.7	51.5	13.4	27.8	3.6

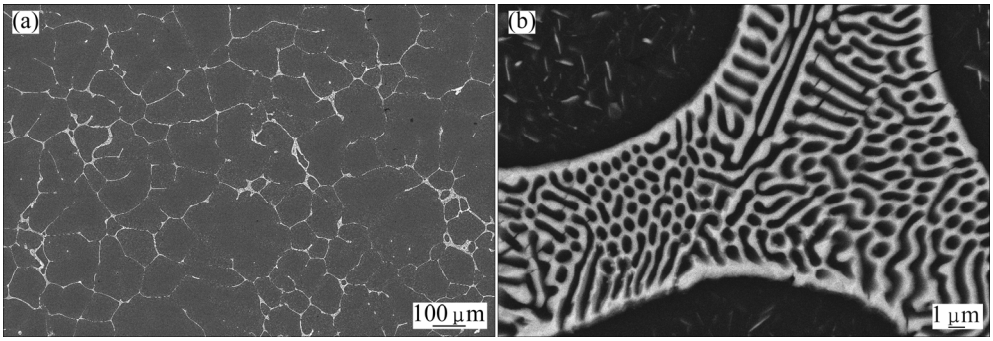

Fig. 3 Microstructures of as-cast 7B04 alloy: (a) Dendritic structure; (b) Secondary phases

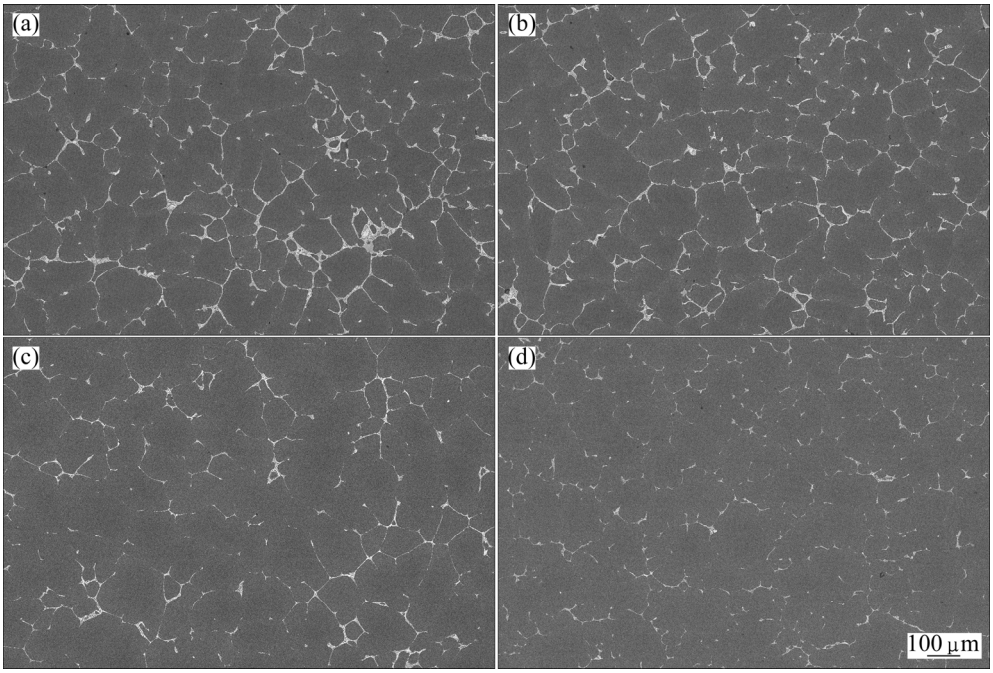

Fig. 4 FESEM images of different samples: (a) Normal homogenization at 380 °C; (b) DC homogenization at 380 °C; (c) Normal homogenization at 465 °C; (d) DC homogenization at 465 °C

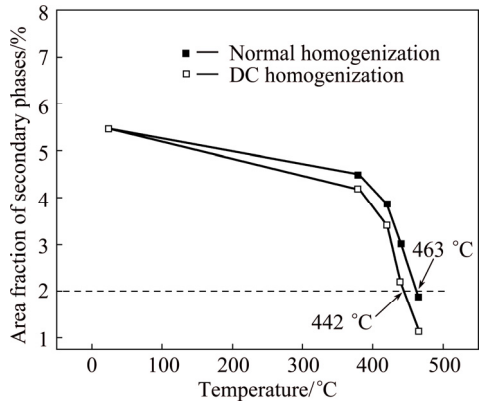

Fig. 5 Area fractions of secondary phases in homogenized samples at 380−465 °C

related technological interest of DC in homogenization depends on its energy saving. It can be deduced from Fig. 5 that, the homogenization temperature to achieve an area fraction of secondary phase of 2.0% is 463 °C for normal homogenized sample and 442 °C for DC homogenized sample. Therefore, in the view of reducing homogenization temperature, the application of DC during homogenization is expected to be used in industrial production to reduce processing costs and/or improve mechanical properties.

Back scattered electron images (Fig. 6) illustrate the changes in morphologies of *T* and *S* phases in homogenized alloys. The white, gray and dark gray contrasts can be clearly seen within *T* phase in alloys under all conditions. When temperature increases from

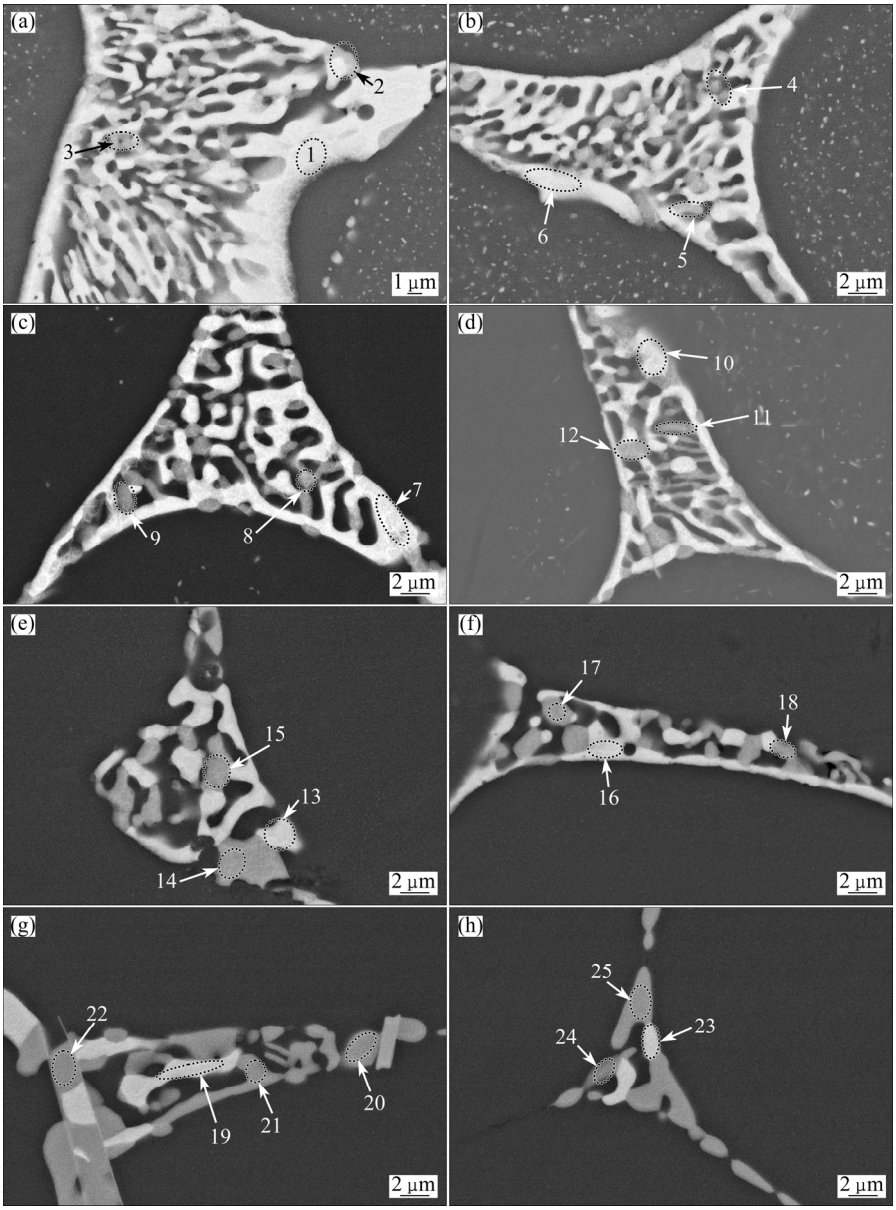

Fig. 6 Back scattered electron images showing morphologies of *T* and *S* phases in as-cast and homogenized alloys: (a) Normal homogenization at 380 °C; (b) DC homogenization at 380 °C; (c) Normal homogenization at 420 °C; (d) DC homogenization at 420 °C; (e) Normal homogenization at 440 °C; (f) DC homogenization at 440 °C; (g) Normal homogenization at 465 °C; (h) DC homogenization at 465 °C

380 to 465 °C, the amount and size of white phase gradually decrease, while the amount of gray phase increases, and some gray phases become coarse at temperature ≥440 °C (Figs. 6(e)−(h)). The amount of gray phase increases with the application of DC at the same temperature (Figs. 6(b), (d), (f) and (h)).

Changes in compositions of white, gray and dark gray phases (labeled as 1−25 in Fig. 6) in homogenized alloys are given in Table 2. The bright white phase normally contains 13.9%−18.6% Mg, 20%−35% Al, 19.3%−28.6% Cu and 29.4%−33.8% Zn (mass fraction), which is similar to that of *T* phase in as-cast alloy, and its composition changes little with the change of temperature. The gray and dark gray phases have compositions (mass fraction) of 11.5%−16.9% Mg, 37%−49.1% Al, 23%−40.3% Cu, 4.8%−16.4% Zn and 12%−15.7% Mg, 36.9%−51.7% Al, 26.5%−44.9% Cu, 2.5%−9.8% Zn, respectively. The compositions of *T* and *S* phases reported in the literatures are listed in Table 3. It can be seen that the composition of *T* phase obtained in present work is close to that obtained by MONDAL and MUKHOPADHYAY [4], which does not agree well with those reported in other research works [2,7,13,14]. The composition of dark gray phase in present work is close to those of *S* phase acquired by other researchers [2,6,13,15]. Phases with different contrasts are divided by Zn content in this work: *T* phase (≥25% Zn), *T*-base phase (≥10% Zn), *S*-base phase (≥3% Zn) and *S* phase (<3% Zn), which is arranged in order of increasing Cu content. The difference in compositions between the gray and dark gray phases reduces with increasing temperature. It can be seen that Zn content in gray or dark gray phases decreases further in DC homogenized samples, which indicates that DC accelerates the transformation from white *T* phase to gray phase and then to dark gray phase. According to the results of EDS analysis, no obvious changes in Mg and Cu contents can be found in gray or dark gray phases in normal and DC

Table 2 Chemical compositions of secondary phases in homogenized 7B04 alloy at 380−465 °C

Homogenized condition	Phase No. labeled in Fig. 6	Mass fraction/%					Phase contrast	Closest phase
		Mg	Al	Fe	Cu	Zn		
Normal homogenization at 380 °C	1	16.7	26	−	25.2	32.1	Bright white	*T*
	2	11.5	49.1	−	23	16.4	Gray	*T*-base
	3	12	51.7	−	26.5	9.8	Dark gray	*S*-base
DC homogenization at 380 °C	4	15.3	26.2	−	25.6	32.9	Bright white	*T*-base
	5	11.5	46.3	−	27.8	14.4	Gray	*T*-base
	6	14.6	48.8	−	27	9.6	Dark gray	*S*-base
Normal homogenization at 420 °C	7	18.5	20	−	28.6	32.9	Bright white	*T*
	8	16.9	42	−	27.8	13.3	Gray	*T*-base
	9	14.3	42.7	−	34.3	8.7	Dark gray	*S*-base
DC homogenization at 420 °C	10	16.2	30	−	21.3	32.5	Bright white	*T*-base
	11	14.3	47.1	−	27.4	11.2	Gray	*T*-base
	12	14.6	47.2	−	31.1	7.1	Dark gray	*S*-base
Normal homogenization at 440 °C	13	18.6	24.1	−	27.9	29.4	Bright white	*T*
	14	14.3	37	−	40.3	8.4	Gray	*S*-base
	15	14.1	50.5	−	30.2	5.2	Dark gray	*S*-base
DC homogenization at 440 °C	16	14.2	35	−	19.3	31.5	Bright white	*T*
	17	15.1	43.8	−	33.5	7.6	Gray	*S*-base
	18	14.4	41	−	40.3	4.3	Dark gray	*S*-base
Normal homogenization at 465 °C	19	13.9	38.1	−	20.2	27.9	Bright white	*T*
	20	11.5	51.2	−	32.2	5.2	Gray	*S*-base
	21	13.7	47.6	−	35.7	2.9	Dark gray	*S*
	22	2.7	62.3	6.6	28.4	−	Bright gray	Al_7Cu_2Fe
DC homogenization at 465 °C	23	15.9	25.8	−	24.6	33.8	Bright white	*T*-base
	24	14.2	48.8	−	32.2	4.8	Gray	*S*-base
	25	15.7	36.9	−	44.9	2.5	Dark gray	*S*

Table 3 Chemical compositions of *T* and *S* phases reported in literatures

Aluminum alloy	Phase	Mg	Al	Cu	Zn
Al−8Zn−7Mg−2Cu [2]	*T* (mass fraction, %)	22.1−23.9	25.5−27.2	13.1−17.6	34.9−36.8
7055 [4]	*T* (mass fraction, %)	19.1−21.1	15.3−20.2	24.8−26	33.5−37.6
7055 [7]	*T* (mass fraction, %)	35	26	16	23
7B04 [13]	*T* (mole fraction, %)	32.4	26.7	20.4	20.5
Al−10Zn−2.5Mg−2.5Cu [14]	*T* (mole fraction, %)	33.7−34.4	14.2−14.7	10.5−14.9	34−41.3
Al−8Zn−7Mg−2Cu [2]	*S* (mass fraction, %)	16−17.1	40.3−47	34.1−39.7	2.7−3.2
7050 [3]	*S* (mole fraction, %)	18.2	59.3	20.4	2.1
7055 [6]	*S* (mole fraction, %)	15.3	57.7	19.7	7.3
7B04 [13]	*S* (mole fraction, %)	21.3	58.1	20.6	−
7050 [15]	*S* (mole fraction, %)	19.1−28	48.9−61.6	18.2−18.6	0.6−4.7

homogenized samples at the same temperature.

4 Discussion

4.1 Effects of DC on electric conductivity and hardness of alloys during homogenization

In present work, with increasing temperature and applying DC, the hardness of the sample increases, but the electric conductivity decreases. The DC homogenized sample has higher hardness and lower electric conductivity at the same temperature. According to SEM observations, smaller size and area fractions of secondary phase are detected in DC homogenized sample.

Accompanying the dissolution of the secondary phase, it becomes spheroidizing, at the same time, the size and the area fraction of it decrease. It is well known that the amount of the element coming into the matrix can be characterized by the hardness and electric conductivity. With increasing the amount of element in the matrix, the harness increases, but the electric conductivity decreases. More alloying elements Zn, Mg and Cu come into the α(Al) matrix due to the accelerated dissolution of secondary phases by applying DC, and thus hardness is greatly improved due to solid solution hardening [16]. The electric conductivity of the Al−Zn−Mg−Cu alloy is related to the amount of the solute atoms remaining in the Al matrix, which means that the more the solute atoms dissolved in Al matrix, the lower the electric conductivity can be obtained. The reason is that the solute atoms in matrix can not only act as the obstacles to the movement of conduction electron, but also increase the density of electron scattering centers-lattice imperfections [17]. Because DC promotes more solute atoms to dissolve in α(Al) matrix, the electric conductivity decreases in DC homogenized sample.

4.2 Effects of DC on evolution of compositions of *T* and *S* phases during homogenization

Changes in main elemental distribution of Mg, Zn and Cu in secondary phases in normal and DC homogenized samples at 440 °C are displayed in Fig. 7. Numerous Mg and Zn can be seen in the matrix neighboring secondary phases in Figs. 7(a), (b), (d) and (e). It should be noted that little Cu can be found in the matrix neighboring secondary phases in Figs. 7(c) and (f), while a diffusion layer of Cu (circle region) is clearly seen at the margin of *T* phase in normal homogenized sample (Fig. 7(c)), and becomes significant in DC homogenized sample (Fig. 7(f)).

In order to investigate effects of DC on the elemental diffusion of *T* phase, the compositions from *T* phase at grain boundaries to grain interior at a distance of 2 μm were measured by EDS analysis in normal and DC homogenized samples at 440 °C. The composition of *T* phase normally falls in a range, and also varies between different positions in one sample or samples homogenized under different conditions, so the deviation in composition between each position and the matrix in one sample can be used to evaluate the elemental diffusion during homogenization, and is illustrated in Fig. 8. The peaks of Cu, Mg and Zn are found at position of 4 μm from *T* phase in normal homogenized sample at 440 °C, which indicates the significant diffusion of these elements during homogenization. It should be noted that the contents of Mg, Cu and Zn are higher in DC homogenized sample at the same distance, and the peaks of Cu, Mg and Zn are found at 8, 8 and 6 μm, respectively, which indicates that these elements diffuse further with the help of DC. DU et al [18] summarized and evaluated the diffusion of Cr, Mn, Fe, Ni, Cu, Zn, Mg and Si in FCC Al alloys. It is found that the diffusion activation energy of Zn is close to that of Mg, and much lower than that of Cu; while Mg has the smallest

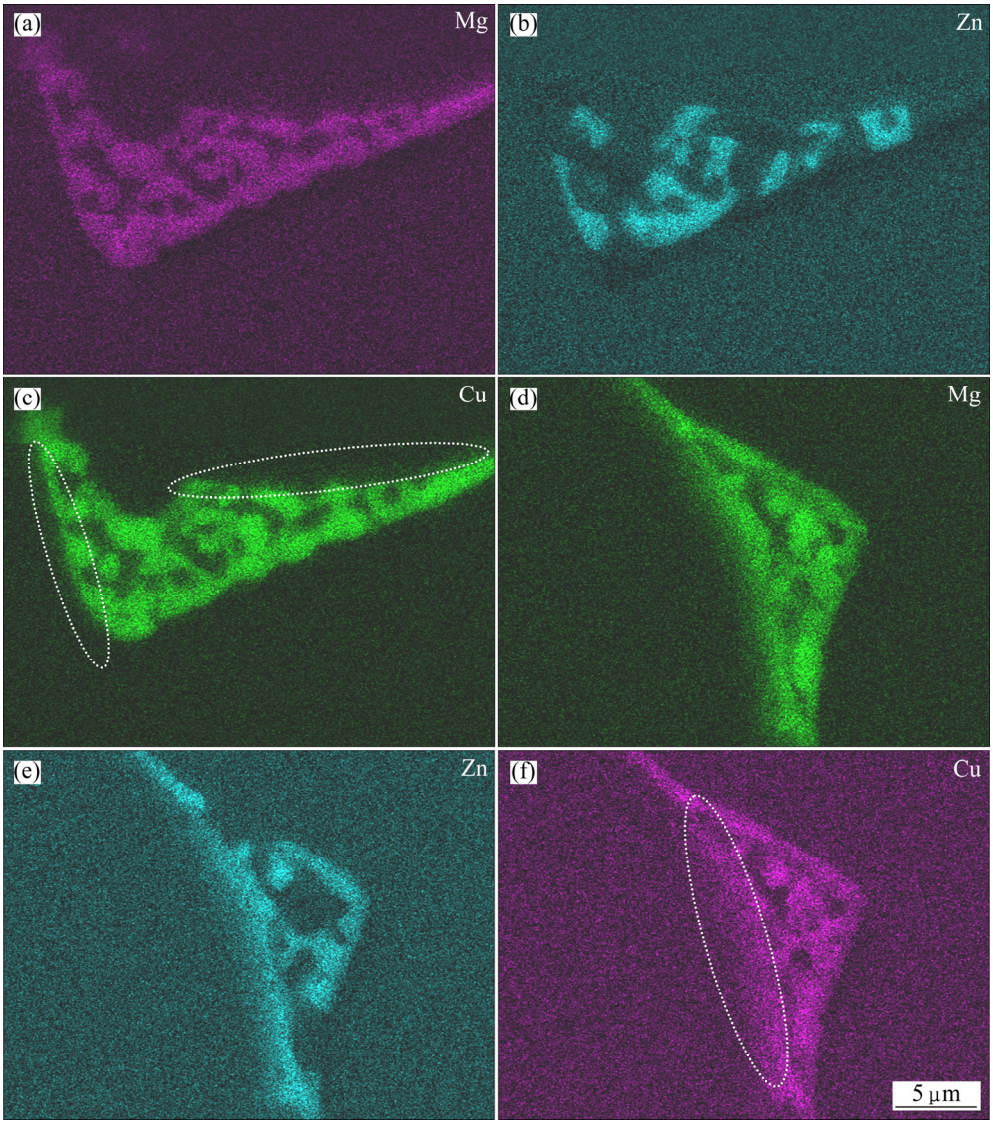

Fig. 7 Elemental distribution of Mg, Zn and Cu in alloys homogenized at 440 °C for 2 h: (a)−(c) Normal homogenized samples; (d)−(f) DC homogenized samples

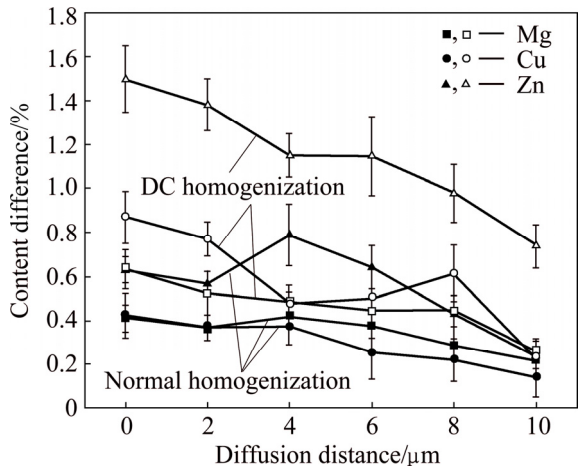

Fig. 8 Differences in contents of Zn, Cu and Mg between each position and matrix from *T* phase to grain interior at distance of 2 μm in homogenized samples at 440 °C

diffusion coefficient among them. According to the above observations, it can be deduced that the diffusion velocity of Zn is much faster than those of Mg and Cu, and DC obviously accelerates the diffusion of Zn and Cu in 7B04 alloy during homogenization. LIU and CUI [19] investigated the effects of applying an electric field (E=2 kV/cm) during the homogenization on the microstructures and mechanical properties of 2091 alloy during the subsequent aging at 180 °C. They found that the electric field increased the yield strength of the alloy by a much more homogeneous and finer precipitation.

4.3 Mechanism of DC effects on dissolution of secondary phase during homogenization

There exist different theories and experimental results about the mechanism of the influence of the electric current. LIU et al [20] investigated the effect of the electric field on the homogenization of Al−Li alloy,

and thought that a charge might be generated on the defects (vacancies or dislocations) due to the perturbation of the electronic state at these defects. The applied field created a charged surface layer in metallic materials and the interaction of the surface charge with the charged defects, particularly vacancies, and thus an additional vacancy flux was created when it approached the specimen surface. Accompanying the dissolution of second phase particles toward the grain interior, the complexes migrated to grain boundaries. JUNG and CONRAD [21] found that the effect of an electric field on the solubility in several Al−Mg−Si alloys changed linearly with the difference in valence between Al matrix and relevant solute atom.

According to the previous works, the mechanism of the DC acting on the homogenization of an Al−Zn−Mg−Cu alloy could be suggested: an equilibrium concentration of vacancies is generated and distributed throughout the lattice due to the high-temperature homogenization. The solute atoms diffuse toward the grain interior because of a high concentration gradient of solute atoms, but vacancies migrate to grain boundaries according to the vacancy mechanism, which leads to the dissolution of second phase particles. The electromigration and the ponderomotive force caused by DC promote the mobility of vacancy during homogenization. The DC reduces the energy barrier which should be overcome during the process of solute atom dissolution of secondary phase, as a result, the diffusibility of solute atoms is promoted and the phase transformation and dissolution are enhanced. However, to disclose the mechanism of DC effects, detailed work should be carried out in the future.

5 Conclusions

1) The conductivity of the 7B04 alloy decreases to 34.9%IACS, the hardness increases to HV 96, and the area fraction of the secondary phase decreases by 6.7%, when the as-cast alloy is DC homogenized at 380 °C. The conductivity and the area fraction of the secondary phase of DC homogenized sample are lower, but hardness is higher than those of normal homogenized sample at the same temperature.

2) The application of DC accelerates the transformation from white *T* phase to gray phase and then to dark gray phase. The gray phase becomes coarse and the deviation in compositions between the gray and dark gray phases reduces when the temperature is not lower than 440 °C.

3) With the application of DC, the diffusion of Zn from *T* phase to grain interior during homogenization is accelerated significantly, and the diffusion of Cu above 440 °C becomes obvious.

References

[1] LI Zhi-hui, XIONG Bai-qing, ZHANG Yong-an, ZHU Bao-hong, WANG Feng, LIU Hong-wei. Microstructural evolution of aluminum alloy 7B04 thick plate by various thermal treatments [J]. Transactions of Nonferrous Metals Society of China, 2008, 18(1): 40−45.

[2] ROKHLIN L L, DOBATKINA T V, BOCHVAR N R, LYSOVA E V. Investigation of phase equilibria in alloys of the Al−Zn−Mg−Cu−Zr−Sc system [J]. J Alloys Compd, 2004, 367: 10−16.

[3] ROBSON J D. Microstructural evolution in aluminum alloy 7050 during processing [J]. Mater Sci Eng A, 2004, 382: 112−121.

[4] MONDAL C, MUKHOPADHYAY A K. On the nature of *T* ($Al_2Mg_3Zn_3$) and *S* (Al_2CuMg) phases present in as-cast and annealed 7055 aluminum alloy [J]. Mater Sci Eng A, 2005, 391: 367−376.

[5] WANG H J, XU J, KANG Y L, TANG M G, ZHANG Z F. Study on inhomogeneous characteristics and optimize homogenization treatment parameter for large size DC ingots of Al−Zn−Mg−Cu alloys [J]. J Alloys Compd, 2014, 585: 19−24.

[6] FAN Xi-gang, JIANG Da-ming, MENG Qing-chang, ZHANG Bao-you, WANG Tao. Evolution of eutectic structures in Al−Zn−Mg−Cu alloys during heat treatment [J]. Transactions of Nonferrous Metals Society of China, 2006, 16(3): 577−581.

[7] CHEN K H, LIU H W, ZHANG Z, LI S, TODD R I. The improvement of constituent dissolution and mechanical properties of 7055 aluminum alloy by stepped heat treatments [J]. Mater Process Tech, 2003, 142: 190−196.

[8] LIU W, CUI J Z. A study on the ageing treatment of 2091 Al−Li alloy with an electric field [J]. Mater Sci Lett, 1997, 16: 1410−1411.

[9] CONRAD H. Effects of electric current on solid state phase transformations in metals [J]. Mater Sci Eng A, 2000, 287: 227−237.

[10] ZHOU Ming-zhe, YI Dan-qing, YIN De-yan, HONG Tian-ran, HUANG Dao-yuan. Effect of electric field on kinetics of formation of S phase in 2E12 aluminum alloy [J]. The Chinese Journal of Nonferrous Metals, 2010, 20(7): 1290−1293. (in Chinese)

[11] HE L Z, LI X, ZHU P, CAO Y H, GUO Y P, CUI J Z. Effects of high magnetic field on the evolutions of constituent phases in 7085 aluminum alloy during homogenization [J]. Mater Charact, 2012, 71: 19−23.

[12] JIA P F, CAO Y H, GENG Y D, HE L Z, CUI J Z. Studies on the microstructures and properties in phase transformation of homogenized 7050 alloy [J]. Mater Sci Eng A, 2014, 615: 335−342.

[13] LI Nian-kui, CUI Jian-zhong. Microstructural evolution of high strength 7B04 ingot during homogenization treatment [J]. Transactions of Nonferrous Metals Society of China, 2008, 18(4): 769−773.

[14] LI Y X, LI P, ZHAO G, LIU X T, CUI J Z. The constituents in Al−10Zn−2.5Mg−2.5Cu aluminum alloy [J]. Mater Sci Eng A, 2005, 397: 204−208.

[15] DENG Y, YIN Z M, CONG F G. Intermetallic phase evolution of 7050 aluminum alloy during homogenization [J]. Intermetallics, 2012, 26: 114−121.

[16] FERGUSON J B, SCHULTZ B, MANTAS J C, SCHOKOUHI H, ROHATGI P K. Effect of Cu, Zn, and Mg concentration on heat treating behavior of squeeze cast Al−(10 to 12)Zn−(3.0 to 3.4)Mg−(0.8 to 1)Cu [J]. Metals, 2014, 4: 314−321.

[17] BATAWI E, MORRIS D G, MORRIS M A. Effect of small alloying additions on behavior of rapidly solidified Cu−Cr alloys [J]. Mater Sci Technol, 1990, 6: 892−899.

[18] DU Y, CHANG Y A, HUANG B Y, GONG W P, JIN Z P, XU H H, YUAN Z H, LIU Y, HE Y H, XIE F Y. Diffusion coefficients of some solutes in FCC and liquid Al: Critical evaluation and correlation [J].

Mater Sci Eng A, 2003, 363: 140−151.
[19] LIU W, CUI J Z. Effect of the homogenization treatment in an electric field on T_1 precipitation in 2091 Al−Li alloy [J]. Scr Metall Mater, 1995, 33: 623−626.
[20] LIU W, LIANG K M, ZHENG Y K, CUI J Z. Study of the diffusion of Al−Li alloys subjected to an electric field [J]. J Mater Sci, 1998, 33: 1043−1047.
[21] JUNG K, CONRAD H. External electric field applied during solution heat treatment of the Al−Mg−Si alloy AA6022 [J]. J Mater Sci, 2004, 39: 6483−6486.

7B04 铝合金直流电均匀化过程中的第二相和性能演化

何立子[1]，贾品峰[1]，张 林[2]，崔建忠[1]

1. 东北大学 材料电磁过程研究教育部重点实验室，沈阳 110819；
2. 东北大学 材料科学与工程学院，沈阳 110819

摘 要：采用电导率测量、硬度测试、X 射线衍射分析、场发射扫描电镜观察和能谱分析方法，研究直流电对 7B04 铝合金在 380~465 °C 均匀化 2 h 后的硬度和第二相形貌演化的影响。结果表明，当温度从 380 °C 升高至 465 °C 时，无电流均匀化试样的电导率由 34.9% IACS 降低至 28.7% IACS，硬度由 HV 96 增加至 HV 146，第二相的面积分数由 4.5%减小至 1.89%。在相同温度下，经直流电均匀化的试样具有较高的硬度、较低的电导率和较小的第二相面积分数。直流电通过促进溶质原子扩散能力和空位的可动性使均匀化效果增强。

关键词：7B04 合金；直流电；均匀化；第二相；元素扩散

(Edited by Wei-ping CHEN)